ROBUST POSITION CONTROL OF LINEAER PIEZOELECTRIC MOTOR DRIVE SYSTEMS

Xin Qian* **Youyi Wang***

**School of Electrical and Electronic Engineering*
Nanyang Technological University, Singapore 639798

Abstract: The friction and load variation are the main uncertainties in the linear piezoelectric motor system. Only the viscous friction is considered in previous work, but it is quite different with the practical condition. Highly nonlinear friction in the system is measured and compensated by a radial basis function (RBF) network. A discrete-time sliding mode controller, which is insensitive to the perturbed state matrix and input matrix and disturbances, is proposed for LPM drive system. Furthermore, three free design parameters are optimized to achieve better transient performance by genetic algorithm and one online mass estimator is adopted to extend the robustness. The simulation and experiment results show that the proposed controller has a stronger robustness than PID controller.

Keywords: Linear motors, Radial base function networks, Discrete-time, Sliding mode control, Genetic algorithms

1. INTRODUCTION

Electromagnetic motors have actually dominated the industry for more than a hundred years. In recent years, a variety of novel types of piezoelectric motors have attracted special interest as new operating principle-based servo actuators in the field of precision motion control applications. The piezoelectric motor can be called a milestone of new generation motor, which has totally different operating principle from the electromagnetic motor counterpart. The first applied linear piezoelectric motor (LPM) appeared in the 1970s (Bansevichyus, *et al.*, 1978). Different construction and driving principles of LPM have been reported (Sachida, *et al.*, 1993; Hu, *et al.*, 2001). The precise motion control of the LPM drive system requires detailed system model. However, the system mathematic model is so complex and the motor parameters are influenced by the uncertainties and disturbances. Friction and mass variations are the main concern in LPM drive system. Several friction models and parameter measurement methods have been addressed for adequate friction compensation (Canudas, *et al.*, 1997). However, the parameter measurement always requires special hardware design or extra hardware requirement. Load variations problem in the system can be solved by two ways. One is to resort to the robust controller, the other is to resort to the load estimator.

During the last two decades, variable structure control (VSC) has gained significant interests and gradually applied in the industrial applications. A reaching law based approach for designing the DSM control law is proposed. However, many works on DSM control only deal with exogenous disturbance and matching condition, where friction is lumped into system uncertainties and the nonlinear dynamic characteristic of friction cannot be compensated effectively.

The paper is organized as follow, in section 2 the structure and model of the LPM are introduced briefly, followed by the system identification of the system with nonlinear friction compensation. In section 4, one novel sliding mode controller is proposed with Genetic algorithm based parameter optimization. Simulation and experiment results are

also demonstrated to validate the effectiveness of the proposed control scheme in section 5.

2. MODEL OF THE LINEAR PIEZOELECTRIC MOTOR

2.1 Principle and Structure of LPM

The inverse piezoelectric effect in piezoceramics converts electrical field to mechanical strain. Under special electrical excitation drive and ceramic geometry of piezoelectric motors, longitudinal extension and transverse bending oscillation modes are excited at close frequency proximity. The simultaneous excitation of the longitudinal extension mode and the transverse bending mode creates a small elliptical trajectory of the ceramic edge, thus achieving the dual mode standing wave motor. By coupling the ceramic edge to a precision stage, a resultant driving force is exerted on the stage, causing stage movement. Fig. 1 shows the basic structure of the linear piezoelectric motor.

2.2 Control model of LPM

The linear piezoelectric motor used in the project is from the Nanomotion. This kind of motor is driven by a high-frequency (39.6kHz) sine wave voltage, which is generated by an inverter operating over the resonance frequency. The motor and drive can be modeled as a DC motor with friction driven by a voltage amplifier. The motion system is modeled as follow:

$$m\ddot{y} = K_f u - K_{fv}\dot{y} - f(\dot{y}) \qquad (1)$$

K_{fv} is the viscosity constant. K_f is electrical-mechanical energy conversion constant. u is the V_{in}, command voltage to the driver which is from the output of controller. The $f(\dot{y})$ is the highly nonlinear friction in the system and will be compensated by a radial basis function (RBF) in the paper.

3. SYSTEM IDENTIFICATION OF LPM DRIVE SYSTEM

3.1 System Configuration

The experimental components consist of DC power source, LPM (it is such a small one but it can drive a big stage as shown in Fig. 2), motor driver, position encoder, dSPACE DS1103 card and dynamic signal analyzer. The experiment platform is shown in Fig. 2.

3.2 Basis Function Compensation for Friction

An RBF network can be described by the following equations.

$$F(x) = w_0 + \sum_{i=1}^{m} w_i \varphi_i(\|x - c_i\|) \qquad (2)$$

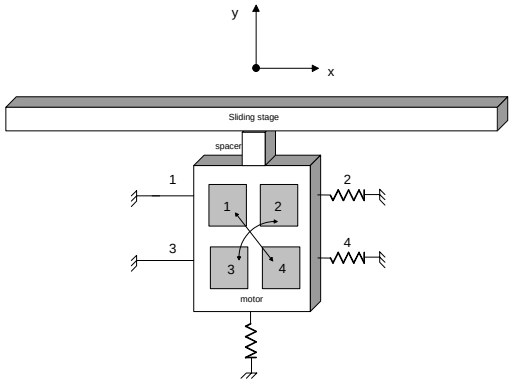

Fig. 1 Structure of the linear piezoelectric motor from Nanomotion

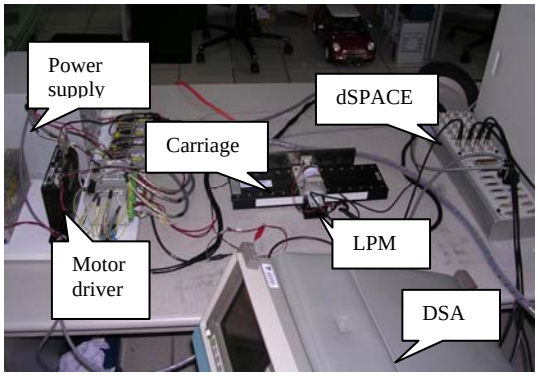

Fig. 2 The overall experimental system

where x is the input vector, $\{\varphi_i(.)\,|\,i = 1, 2, ..., m\}$ is the set of basis functions. w_i are the weights, c_i, are known as the RBF center, and m is the number of centers. In the RBF network, the functional form φ(.) and c_i are assumed to have been fixed.

The RBF adopted in the paper is given by:

$$\varphi_i(\|x - c_i\|) = \exp(-\frac{\|x-c_i\|^2}{2\sigma^2}) \qquad (3)$$

where σ is a parameter which indicates how the RBF response increases when input state approaches the center c_i.

An orthogonal least squares (OLS) procedure proposed by (Chen, *et al*. 1991) chooses the centers of the RBFs as subsets of the weighting matrix from a linear regression model of the error equation.

$$d^i = \sum_{j=1}^{m} \varphi_j(\|x^i - c_j\|) w_j + e^i \qquad i: 1, 2, ..., n \qquad (4)$$

In the regression model, d^i is the desired response, φ are the regressors, w_j are the parameters, and e^i are the residual errors. The vector expression of the equation can be shown as:

$$D = \Phi W + E \qquad (5)$$

OLS transforms the columns of ϕ into a set of orthogonal vectors ϕ=QR. Then, the equation is represented as:

$$D = QRW + E = Qg + E \qquad (6)$$

Q are the sets of orthogonal vectors, the squares D can be obtained by:

$$D^T D = \sum_{j=1}^{m} g_j^2 Q_j^T Q_j + E^T E \qquad (7)$$

Thus, an error reduction ratio due to Q is defined as:

$$[err]_j = \frac{g_j^2 Q_j^T Q^T}{D^T D},\ j:1,2,...,m \tag{8}$$

The ratio can be applied to rank the RBFs according to their contribution to the reduction of the approximation error. The regressor selection procedure is terminated at the sth step when

$$1-\sum_{j=1}^{s}[err]_j < \rho \tag{9}$$

where $0<\rho<1$ is the chosen tolerance. Here, ρ is chosen as 0.001.

Since the accurate parameter values in (1) are difficult to obtain, Dynamic signal analyzer (DSA) is first used to identify the system.

The system model can be measured by DSA directly under the nonlinear friction compensation. The bode diagram of the plant with 0kg payload is shown in Fig. 3. The curve fitting can be fulfilled by Dynamic Signal Analyzer (DSA).

The curve fitting plant model for 0kg payload is:

$$\frac{Y(s)}{U(s)} = \frac{10.25}{s(s+30.025)} \tag{10}$$

In the same manner, the models for 3.5kg and 7kg payloads are as follow:

$$\frac{Y(s)}{U(s)} = \frac{5.27}{s(s+15.43)} \text{ and } \frac{Y(s)}{U(s)} = \frac{3.54}{s(s+10.382)} \tag{11}$$

4. ROBUST CONTROLLER DESIGN

To solve the large parameter variations and nonlinear compensation problem in LPM drive system, the whole control structure is proposed and shown in Fig. 4. The mass estimator is achieved based on estimation algorithm named recursive least square with forgetting factor (Ljung, 1999). The GA based sliding mode controller is to be described in details.

4.1 Discrete Time Sliding Mode Control

The motion system is modeled as (1)

$$m\ddot{y} = K_f u - K_{fv}\dot{y} - f(\dot{y}) \tag{12}$$

that is, $$\ddot{y} = \frac{1}{m}(K_f u - K_{fv}\dot{y} - f(\dot{y})) \tag{13}$$

It can be shown in standard state-space form:

$$\begin{aligned} \dot{y} &= v \\ \dot{v} &= -k_{fv}v/m + k_f u/m - f(v)/m \end{aligned} \tag{14}$$

The system will be digitalized in the practical application by computer-aim method. Thus, denote

$$\begin{aligned} &y_k = y(kT_s), v = v(kT_s), \dot{v} = (v_{k+1} - v_k)/T_s \\ &\text{and } f = \begin{bmatrix} 0 & -T_s f(kT_s)/m \end{bmatrix}^T \end{aligned} \tag{15}$$

where T_s is the sampling time. The system is transformed to discretization system by the forward Euler method.

$$\begin{aligned} x_{k+1} &= \Phi x_k + \Gamma u_k + f \\ y_k &= C x_k \end{aligned} \tag{16}$$

where

$$x_k = \begin{bmatrix} y_k \\ v_k \end{bmatrix}, \Phi = \begin{bmatrix} 1 & T_s \\ 0 & 1 - T_s k_{fv}/m \end{bmatrix},$$
$$and\ \Gamma = \begin{bmatrix} 0 \\ T_s k_f/m \end{bmatrix}, C = [1 \quad 0] \tag{17}$$

The friction function and the mass are time varying and uncertain parameters of the system. However, the extent of the parameter is bounded by known. The control problem is to make the state x_k track a specific time varying state x_d under the time varying friction and mass.

Let us define a sliding surface by the scalar equation $S_k = 0$,

$$\text{where, } S = \{ s_k \,|\, s_k = \Lambda(x_k - x_k^d) = 0,\ k = 0,1,...,s(kT_s) = s_k \} \tag{18}$$

where, $\Lambda = [\lambda \quad 1]$, λ is a positive real number and $x_k^d = [y_k^d \quad v_k^d]^T$ is the reference input.

Given the initial condition $x(0)=x_d(0)$, the problem of tracking $x \equiv x_d$ is equivalent to that of remaining on the surface S_k for all $k>0$. Thus, the problem of tracking the x_d can be reduced to that of keeping the scalar quantity s at zero.

Adopting the reaching law (Gao, *et al.*, 1993):

$$s_{k+1} - s_k = -QT_s s_k - \eta T_s \operatorname{sgn}(s_k),\ QT_s < 1 \tag{19}$$

$$\begin{aligned} s_{k+1} - s_k &= \Lambda x_{k+1} - \Lambda x_k \\ &= \Lambda(\Phi x_k) + \Lambda(\Gamma u_k) + \Lambda f \\ &\quad - \Lambda x_k - \Lambda(x_{k+1}^d - x_k^d) \end{aligned} \tag{20}$$

solving u from the (19) and (20)

$$\begin{aligned} u_k = -(\Lambda\Gamma)^{-1}[&\Lambda(\Phi x_k) + \Lambda f - \Lambda x_k + QT_s s_k \\ &+ \eta T_s \operatorname{sgn}(s_k)] + \Gamma^{-1}(x_{k+1}^d - x_k^d) \end{aligned} \tag{21}$$

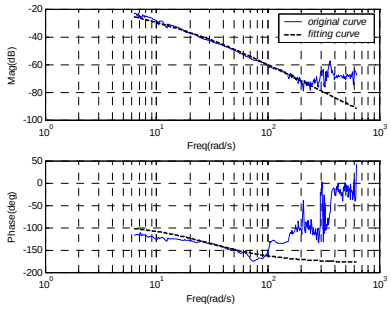

Fig. 3 Bode plot of the system model data for 0kg

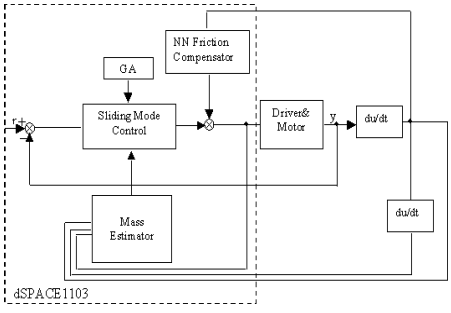

Fig. 4 The structure block diagram of the system

Moreover, $\mathrm{sgn}(1-QT_s s_k)=\mathrm{sgn}(s_k)$ (22)

Then, the sign of s_{k+1} must be opposite to that of s_k according to the definition of quasi-sliding mode (QSM). In the region, every state x satisfies:

$$\left\{x \middle| |s(x)| < \frac{\eta T_s}{1-QT_s}\right\} \quad (23)$$

And the width of the DSM bound is:

$$\Delta = \frac{\eta T_s}{1-QT_s} \quad (24)$$

Consider the system (16) under the unknown mass and friction condition.

$$\begin{aligned} x_{k+1} &= \tilde{\Phi}x_k + \Delta\Phi x_k + \tilde{\Gamma}u_k + \Delta\Gamma u_k + f \\ y_k &= Cx_k \end{aligned} \quad (25)$$

For the current system, the following matching conditions are satisfied:

$$\begin{aligned} \Delta\Phi &= \tilde{\Gamma}\hat{\Phi} \\ \Delta\Gamma &= \tilde{\Gamma}\hat{\Gamma} \\ f &= \tilde{\Gamma}\hat{f} \end{aligned} \quad (26)$$

Consider the system (25), the (21) becomes

$$\begin{aligned} u_k = -(\Lambda\tilde{\Gamma})^{-1}[&\Lambda(\tilde{\Phi}x_k) + \Lambda\tilde{f} - \Lambda x_k + QT_s s_k \\ &+ \eta T_s \,\mathrm{sgn}(s_k)] - \hat{\Gamma}u_k - \hat{\Phi}x_k - \hat{f} \\ &+ \tilde{\Gamma}^{-1}(x_{k+1}^d - x_k^d) \end{aligned} \quad (27)$$

The $\hat{\Phi}, \hat{\Gamma}, \hat{f}$ in (27) are unknown elements, thus, (27) cannot be used to design the controller. Assume $\hat{\Phi}, \hat{\Gamma}, \hat{f}$ can be replaced by the elements Φ_c, Γ_c, f_c, which will be specified by the following procedure.

After the substitution, (27) becomes:

$$\begin{aligned} u_k = -(\Lambda\tilde{\Gamma})^{-1}[&\Lambda(\tilde{\Phi}x_k) + \Lambda\tilde{f} - \Lambda x_k + QT_s s_k \\ &+ \eta T_s \,\mathrm{sgn}(s_k)] - \Gamma_c u_k - \Phi_c x_k - f_c \\ &+ \tilde{\Gamma}^{-1}(x_{k+1}^d - x_k^d) \end{aligned} \quad (28)$$

From the (20) (25) and (28), the incremental change in s_k is expressed:

$$\begin{aligned} s_{k+1} - s_k = &-QT_s s_k - \eta T_s \,\mathrm{sgn}(s_k) - \Lambda(x_{k+1}^d - x_k^d) \\ &+ (\Lambda\tilde{\Gamma})[\hat{\Gamma}u_k - \Gamma_c u_k + \hat{\Phi}x_k - \Phi_c x_k \\ &+ \hat{f} - f_c] \end{aligned} \quad (29)$$

For simplification, let

$$\begin{aligned} \hat{T} = \Lambda\tilde{\Gamma}(\hat{\Gamma}u_k), T_c = \Lambda\tilde{\Gamma}(\Gamma_c u_k) \\ \hat{S} = \Lambda\tilde{\Gamma}(\hat{\Phi}x_k), S_c = \Lambda\tilde{\Gamma}(\Phi_c x_k) \\ \hat{F} = \Lambda\tilde{\Gamma}\hat{f}, F_c = \Lambda\tilde{\Gamma}f_c \end{aligned} \quad (30)$$

Then (29) can be expressed as:

$$\begin{aligned} s_{k+1} - s_k = &-QT_s s_k - \eta T_s \,\mathrm{sgn}(s_k) \\ &+ (\hat{T} - T_c) + (\hat{S} - S_c) + (\hat{F} - F_c) \end{aligned} \quad (31)$$

For the LPM drive system, $\hat{T}$, $\hat{S}$ and $\hat{F}$ have some corresponding relationship with mass and friction of the system itself. They have the upper bound and lower bounds as the mass and friction in the system are not unlimited.

$$T_{\min} \le \hat{T} \le T_{\max}, S_{\min} \le \hat{S} \le S_{\max}, F_{\min} \le \hat{F} \le F_{\max} \quad (32)$$

The value of T_c, S_c and F_c are need to be specified to guarantee the sign of s_{k+1}-s_k is opposite to the sign of s_k, the simple solution is:

$$\begin{cases} T_c = T_{\max}, S_c = S_{\max}, F_c = F_{\max} & \mathrm{sgn}(s_k) = 1 \\ T_c = T_{\min}, S_c = S_{\min}, F_c = F_{\min} & \mathrm{sgn}(s_k) = -1 \end{cases} \quad (33)$$

To formulate (29) as follow:

$$\begin{cases} T_c = (\frac{T_{\max}+T_{\min}}{2}) + (\frac{T_{\max}-T_{\min}}{2})\,\mathrm{sgn}(s_k) \\ S_c = (\frac{S_{\max}+S_{\min}}{2}) + (\frac{S_{\max}-S_{\min}}{2})\,\mathrm{sgn}(s_k) \\ F_c = (\frac{F_{\max}+F_{\min}}{2}) + (\frac{F_{\max}-F_{\min}}{2})\,\mathrm{sgn}(s_k) \end{cases} \quad (34)$$

The final control law is referred from (26) (28) and (34):

$$\begin{aligned} u_k = -(\Lambda\tilde{\Gamma})^{-1}\{&\Lambda(\tilde{\Phi}x_k) - (1-QT_s)s_k \\ &+ \eta T_s \,\mathrm{sgn}(s_k) - \Lambda x_{k+1}^d + (\tfrac{T_{\max}+T_{\min}}{2}) \\ &+ (\tfrac{S_{\max}+S_{\min}}{2}) + (\tfrac{F_{\max}+F_{\min}}{2}) + [(\tfrac{T_{\max}-T_{\min}}{2}) \\ &+ (\tfrac{S_{\max}-S_{\min}}{2}) + (\tfrac{F_{\max}-F_{\min}}{2})] * \mathrm{sgn}(s_k)\} \end{aligned} \quad (35)$$

4.2 Genetic Algorithm Based Parameter Optimization

Three free parameters λ, Q and η exist in the sliding mode control design process. They have been chosen only by experience before. Thus, it is not the optimal one. GA can realize the optimal design with a suitable fitness function.

A fitting function should be set up in order to evaluate the performance of every new generation of the parameters. The fitness function should be suitably designed to incorporate the restrictions. In the paper, the integral of squared error (ISE) of position response is adopted as one part of fitness function. Moreover, the overshoot of the time response is also crucial for the system transient performance. The integral of the overshoot acts as the other part of the fitness function.

$$g = g_{ise} + g_{overshoot} \quad (36)$$

$$g_{ise} = \int_0^T (y(t) - r)^2 dt \quad (37)$$

$$g_{overshoot} = \int_0^T f(y(t)-r)^2 dt, f(x) = \begin{cases} x & x > 0 \\ 0 & x \le 0 \end{cases} \quad (38)$$

The minimization of the evaluation function g is transformed into a maximization search fitness function F by

$$F = \frac{\alpha}{g} \quad (\alpha \text{ is a constant}) \quad (39)$$

Moreover, non-uniform mutation is applied for improving single-element tuning and reducing the disadvantage of random mutation in the float point implementation. Let a_i and b_i be the lower and upper bound, respectively, for each variable i, x_i is an element in the chromosome and x_i' is the next generation of x_i.

$$x_i' = \begin{cases} x_i + (b_i - x_i) f(G) & if\ r_1 < 0.5 \\ x_i - (x_i + a_i) f(G) & if\ r_1 \ge 0.5 \end{cases} \quad (40)$$

where

$$f(G) = (r_2(1 - \frac{G}{G_{\max}}))^b \quad (41)$$

r_1, r_2 : a uniform random number between (0,1)
G : the current generation
G_{max}: the macimum number of generations
b: a shape parameter

The GA moves from generation to generation selecting and reproducing parents until a termination criterion is met.

5. NUMERICAL AND EXPERIMENT RESULTS

5.1 Simulation results

The model used is corresponding to (1):

$$3.7\ddot{y} = 37.925u - 111.1\dot{y} - f(\dot{y}) \quad (42)$$

Φ and Γ in (15) are derived as:

$$\tilde{\Phi} = \begin{bmatrix} 1 & 1.0e-3 \\ 1 & 0.97 \end{bmatrix}, \tilde{\Gamma} = \begin{bmatrix} 0 \\ 0.01 \end{bmatrix}. \quad (43)$$

The unknown parameters in (27) can be further determined:

$$\begin{aligned} &0.17 \le \hat{\Gamma} \le 0.25 \\ &[0 \quad 0.75] \le \hat{\Phi} \le [0 \quad 0.5] \\ &-0.3 \le \hat{f} \le 0.3 \end{aligned} \quad (44)$$

The reference signals in this case are a stepwise change position signal and a swing signal g(t)=sin(t)*sin(10t), which are shown in Fig. 5.

The three parameters λ, Q and η. in (35) are chosen to achieve the optimality with respect to the fitness function (43) based on GA. Specifications of the GA process are the population size of 100, the normalized geometric ranking selection, the one-point crossover with its probability of 0.6, and the non-uniform mutation with its probability of 0.05, respectively. The genetic process is iterated until 200 generations are achieved. After the GA based optimization procedure, the resulting values of them are 78.447, 139.83, 93.763, respectively. The GA based sliding mode controller from (35):

$$\begin{aligned} u_k = &-100\{[79.447 \quad 1.173]x_k + 0.861s_k \\ &-[78.447 \quad 1]x_{k+1}^d + 0.1498\,\mathrm{sgn}(s_k) \\ &+[0 \quad 0.025]x_k\,\mathrm{sgn}(s_k)\} \end{aligned} \quad (45)$$

Fig. 6 ~ Fig. 9 shows the results of position control based on the two methods under different operation conditions. To evaluate the robustness of the proposed control method, the control results are obtained under different frictions and masses. The friction ranges from f_0 to $2f_0$ and the payload ranges from 0kg to 7kg. Under every different condition, the mean tracking error during the whole simulation time is calculated. Fig. 10 shows all the average absolute tracking errors to step reference signal at every

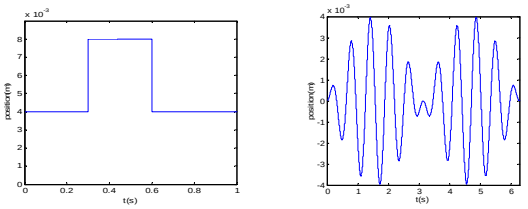

Fig. 5 The reference position signals

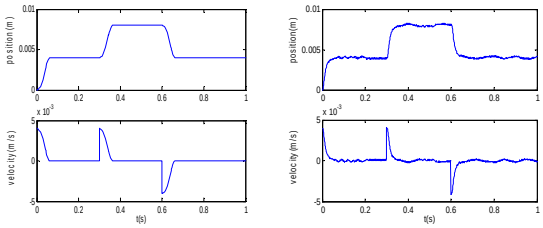

Fig. 6 Tracking performance of proposed method (left) and PID controller (right) under the condition of f=1.2 f_0 and payload m=0kg

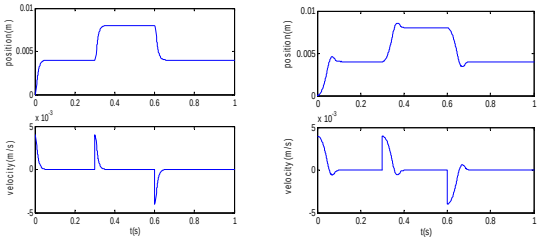

Fig. 7 Tracking performance of proposed method (left) and PID controller (right) under the condition of f=1.2 f_0 and payload m=7kg

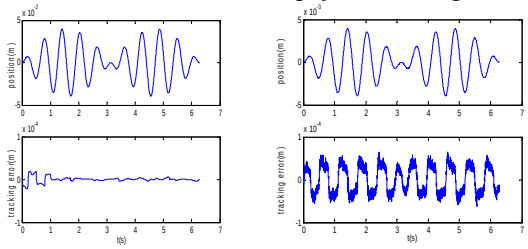

Fig. 8 Tracking performance of proposed method (left) and PID controller (right) under the condition of f=1.2 f_0 and payload m=3.5kg

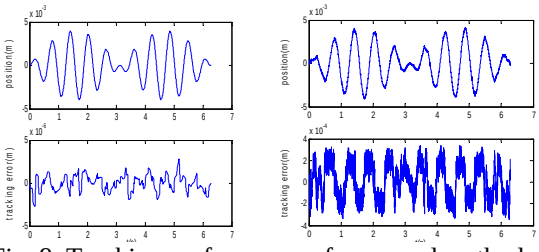

Fig. 9 Tracking performance of proposed method (left) and PID controller (right) under the condition of f=1.2 f_0 and payload m=7kg

point clearly. The tracking error in left picture varies from 1.9E-5 to 1.5E-4. The one in right picture ranges from 2.2E-4 to 5.2E-4.

Hence, the simulation results demonstrate that the proposed controller scheme highly improves the control performance compared with the conventional PID controller.

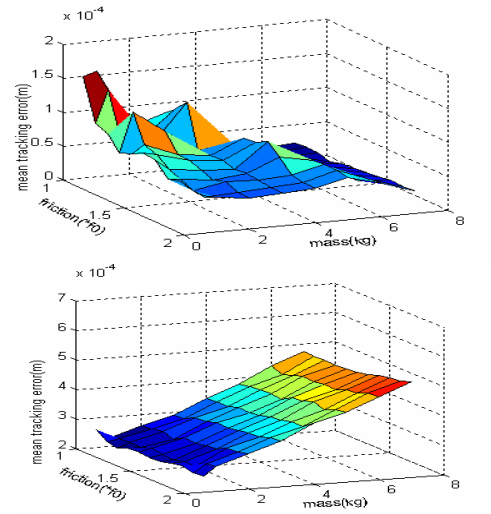

Fig. 10 Mean position tracking error of the proposed method (upper) and PID (lower) with the variations of friction and payload.

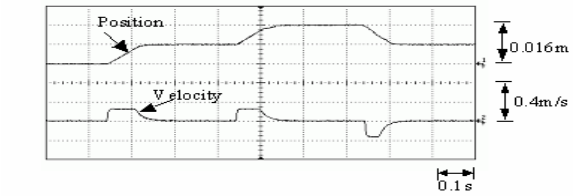

Fig. 11 Experiment stepwise response under payload of 0kg

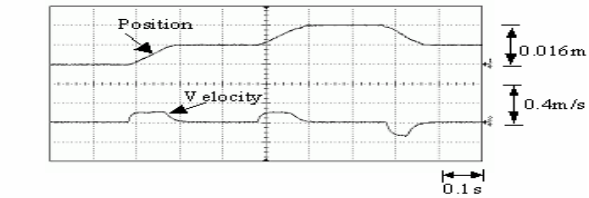

Fig. 12 Experiment stepwise response under payload of 7kg

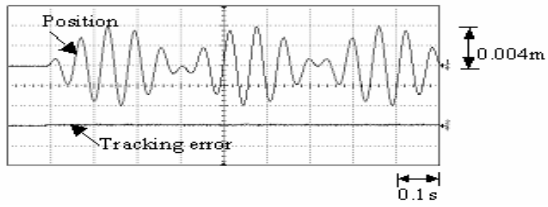

Fig. 13 Experiment swing response under payload of 3.5kg

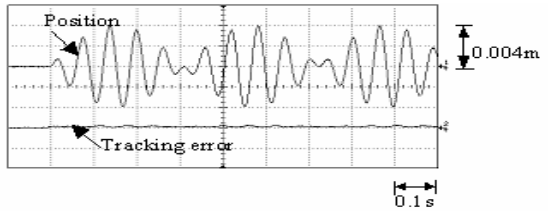

Fig. 14 Experiment swing response under payload of 7kg

5.2 Experiment results

The same controllers are applied in the experimental LPM drive system. The real plant replaces the simulated system model in the experiment. Fig. 11 and Fig. 12 demonstrate the measured carriage stepwise position response under 0kg and 7kg payload and $1.2f_0$ friction condition. Fig. 13 and Fig. 14 demonstrate the swing position response under 3.5kg and 7kg payload and $1.2f_0$ friction condition, respectively. Notably, the experimental results agree with simulated results very well and the controller designed by numerical method provides the same performance in the real-time experiment, which means two things, the controller is practical one and the identified system model from DSA fits the real plant.

6. CONCLUSION

In this paper, a dynamic signal analyzer is first used to identify the LPM drive system and the transfer function of motor together with the driver is obtained. Highly nonlinear friction in the system is measured and compensated by an RBF network. A discrete-time sliding mode controller is designed for the system with perturbed state matrix and input matrix and nonlinear external disturbance based on reaching law approach. In addition, the free parameters in the design process are chosen via genetic algorithm and the least integral of squared error and overshoot of position response is achieved. The large tolerable payload 7kg of the LPM drive system is realized by combined the sliding mode controller and an on-line mass estimator. The simulation results demonstrate that the proposed controller is insensitive to the mass and friction variations and noise and achieves less mean position tracking error and better transient response than PID controller. The experiments are also achieved to validate the effectiveness of the proposed scheme.

REFERENCES

Bansevichyus, R.Y. and K.M. Ragulskis (1978). Vibration motors as precision units for manipulators and robots, *Machines and Tooling*, **49**, 23-27.

Hu, J., G. Li, H. Chan and C. Choy (2001). A standing wave-type noncontact linear ultrasonic motor, *IEEE Trans. Ultrasonics, Ferroelectrics, and Frequency Control*, **48**, 609-708.

Sachida, T. and T. Kenjo (1993). *An Introduction to Ultrasonic Motors*, Clarendon Press, Oxford.

Canudas, C.A. and P. Lischinsky (1997). Adaptive Friction Compensation with Partially Known Dynamic Friction Model *International Journal of Adaptive Control and Signal Processing*, **11,** 65-81.

Chen, S., F.N. Cowan and P. M. Grant (1991). Orthogonal least squares learning algorithm for radial basis function networks, *IEEE Trans. Neural Networks*, **2,** 302-309.

Ljung, L. (1999). *System Identification: Theory for the User*, Prentice-Hall, New Jersey.

Gao, W.B. and J. C. Hung (1993). Variable structure control of nonlinear system: A new approach, *IEEE Trans. Industrial Electronics*, **40**, 45–55.